Mutational Signature 3 Detected from Clinical Panel Sequencing is Associated with Responses to Olaparib in Breast and Ovarian Cancers

Felipe Batalini[1,2,3], Doga C. Gulhan[4], Victor Mao[4], Antuan Tran[4], Madeline Polak[1,5], Niya Xiong[1,6], Nabihah Tayob[1,6], Nadine M. Tung[1,2], Eric P. Winer[1,5], Erica L. Mayer[1,5], Stian Knappskog[7], Per E. Lønning[7], Ursula A. Matulonis[1,8], Panagiotis A. Konstantinopoulos[1,8], David B. Solit[9], Helen Won[9], Hans P. Eikesdal[7], Peter J. Park[4], and Gerburg M. Wulf[1,2]

ABSTRACT

Purpose: The identification of patients with homologous recombination deficiency (HRD) beyond *BRCA1/2* mutations is an urgent task, as they may benefit from PARP inhibitors. We have previously developed a method to detect mutational signature 3 (Sig3), termed SigMA, associated with HRD from clinical panel sequencing data, that is able to reliably detect HRD from the limited sequencing data derived from gene-focused panel sequencing.

Experimental Design: We apply this method to patients from two independent datasets: (i) high-grade serous ovarian cancer and triple-negative breast cancer (TNBC) from a phase Ib trial of the PARP inhibitor olaparib in combination with the PI3K inhibitor buparlisib (BKM120; NCT01623349), and (ii) TNBC patients who received neoadjuvant olaparib in the phase II PETREMAC trial (NCT02624973).

Results: We find that Sig3 as detected by SigMA is positively associated with improved progression-free survival and objective responses. In addition, comparison of Sig3 detection in panel and exome-sequencing data from the same patient samples demonstrated highly concordant results and superior performance in comparison with the genomic instability score.

Conclusions: Our analyses demonstrate that HRD can be detected reliably from panel-sequencing data that are obtained as part of routine clinical care, and that this approach can identify patients beyond those with germline *BRCA1/2*mut who might benefit from PARP inhibitors. Prospective clinical utility testing is warranted.

Introduction

Targeting DNA damage repair with PARP inhibitors (PARPi) has been approved in ovarian, breast, pancreatic, and prostate cancer (1–5). In breast cancer, patients are currently selected on the basis of the presence of a germline *BRCA1/2* pathogenic mutation. However, candidate lesions for PARPi sensitivity include loss-of-function mutations in a large number of other genes, which result in homologous recombination deficiency (HRD), suggesting that testing based only on germline *BRCA1/2*mut may not identify the full set of patients who could benefit from PARPi. In addition, as loss-of-function mutations in these tumor suppressor genes frequently do not occur in hot spots, testing PARPi sensitivity based on the presence of individual mutations in clinical trials is not realistic for the less common HRD genes and may miss cases where HRD is the result of polygenic tumor development (5, 6).

*BRCA1/2*mut and other HRD tumors have been shown to display a specific pattern of genome-wide somatic single nucleotide variations (SNVs) defined as "mutational signature 3" (Sig3) in the COSMIC signature catalog, which consists of several dozen "signatures" based on the base substitution types and the trinucleotide context in which the substitutions occur (7, 8). A pattern of insertions, deletions, and rearrangements have also been associated with *BRCA1/2*mut tumors (8). HRD status can also be inferred from the copy-number variation (CNV) profile of the tumors. For example, a commercial platform for detecting HRD called MyChoice from Myriad Genetics calculates genomic instability score (GIS), comprised of loss-of-heterozygosity (LOH), telomeric allelic imbalance (TAI), and large-scale state transitions (LST; ref. 4). Both Sig3 and GIS are strongly associated with *BRCA1/2* mutations and have been proposed as genomic markers of HRD, and their ability to predict sensitivity to PARPi has been shown in preclinical models (8–14). HRD is also associated with other specific alterations, such as excess of deletions with microhomology at the deletion junction and long tandem duplications. When whole-genome sequencing (WGS) data are available, one could also use the HRDetect diagnostic tool, which utilizes a weighted model that accounts for both substitution and rearrangement signatures to identify HRD cases, even when they are not *BRCA1/2*mut (11).

[1]Harvard Medical School, Department of Medicine, Boston, Massachusetts. [2]Beth Israel Deaconess Medical Center, Division of Medical Oncology and Cancer Research Institute, Boston, Massachusetts. [3]Broad Institute of MIT and Harvard, Cambridge, Massachusetts. [4]Harvard Medical School, Department of Biomedical Informatics, Boston, Massachusetts. [5]Dana-Farber Cancer Institute, Department of Medical Oncology, Boston, Massachusetts. [6]Dana-Farber Cancer Institute, Department of Data Sciences, Boston, Massachusetts. [7]University of Bergen, Department of Clinical Science, Bergen, Norway. [8]Dana-Farber Cancer Institute, Department of Gynecologic Oncology, Boston, Massachusetts. [9]Memorial Sloan Kettering Cancer Center, New York, New York.

P.J. Park and G.M. Wulf contributed equally as the co-senior authors in this article.

F. Batalini and D.C. Gulhan contributed equally as the co-first authors in this article.

Corresponding Authors: Gerburg M. Wulf, Division of Hematology/Oncology, Beth Israel Deaconess Medical Center, Harvard Medical School, Beth Israel Deaconess Medical Center and Department of Medicine, Boston, MA 02215. E-mail: gwulf@bidmc.harvard.edu; and Peter J. Park, 10 Shattuck Street, Boston, MA 02115. E-mail: peter_park@hms.harvard.edu

Clin Cancer Res 2022;28:4714–23

doi: 10.1158/1078-0432.CCR-22-0749

Translational Relevance

Among patients with breast cancer, PARP inhibitors (PARPi) are approved for *BRCA1/2* carriers, but there is growing evidence of benefit in additional patients. There is an immense clinical need for a more comprehensive biomarker of response to PARPi. We have previously developed a method to detect mutational signature 3 (Sig3) associated with homologous recombination deficiency from clinical panel sequencing data. This work brings mutational signatures closer to the clinic by not only confirming our ability to reliably detect Sig3 from clinical sequencing but also relating these to meaningful clinical outcomes (progression-free survival and objective response rate). Our method is unique that it detects Sig3 from routine clinical sequencing (targeting a few hundred genes), whereas previous methods for Sig3 detection required whole-exome or whole-genome sequencing (not routine care). Sig3 could be used to design clinical trials to identify patients who will benefit from PARPi with high probability, without additional sequencing costs.

Clinical validation of these genomic biomarkers of HRD has aimed at identifying patients who might benefit from platinum- or PARPi-based treatment. In breast cancers, LOH and LST scores were associated with platinum responses in the PrECOG 0105 (15) and TBCRC 009 (16) trials. GIS predicted pathologic responses with neoadjuvant chemotherapy (17) and improved disease-free survival with adjuvant epirubicin + cyclophosphamide chemotherapy in SWOG S9313 (18). However, GIS has not been predictive of response in all studies—the Myriad HRD assay was not associated with responses to either neoadjuvant cisplatin or paclitaxel in TBCRC 030 (19) or to docetaxel or carboplatin in the metastatic setting in the TNT trial (20). In ovarian cancers, GIS was associated with progression-free survival (PFS) and overall survival (21). In terms of PARPi, several studies have shown that patients with ovarian cancer with high GIS have longer PFS and higher response rates (1, 4, 22, 23). Instead of using GIS, the ARIEL3 investigators used genome-wide LOH (gLOH) as defined by Foundation Medicine's T5 assay (24) and showed that a gLOH >16% was associated with longer PFS (25).

Other methods for testing HRD status have practical limitations: standard Sig3 detection requires whole-exome sequencing (WES) or WGS data, GIS requires a proprietary assay for profiling *BRCA1/2* mutations and copy-number profiling, and HRDetect requires WGS. In particular, none of these methods could be applied to cancer gene panels (typically 100–400 genes) that are often employed in clinical settings. To overcome this limitation, we have previously developed the Signature Multivariate Analysis (SigMA) algorithm that can infer the presence of Sig3 even when the number of detected mutations is an order of magnitude smaller due to the narrow region of the genome targeted by the panel (14). We initially showed that Sig3 prediction from panels is a good proxy for Sig3 prediction from WES using several cancer cell lines that were treated with PARPi (14). Subsequently, we used SigMA to analyze data from the TOPACIO trial (combination of niraparib with pembrolizumab in ovarian cancer). We showed that Sig3 positivity inferred from panels was associated with response to combined PARP and PD-1 inhibition in ovarian cancer (26).

Here, we assess the validity of panel-based Sig3 (panel-Sig3) prediction by SigMA through a direct comparison with paired WES data as well as with GIS and *BRCA1/2* status on the same tumors. The applicability of panel-Sig3 would be of great clinical importance because it would provide a quicker and much less expensive biomarker in PARPi and other HRD-related clinical studies. We utilized data from a study evaluating the combination of the PI3K inhibitor buparlisib (BKM-120) with olaparib in patients with advanced TNBC or high-grade serous ovarian cancer (HGSOC; ref. 27), where the combined regimen yielded a response rate of 29%. We also externally validated panel-Sig3 using data from the Phase II PETREMAC trial, which investigated single-agent neoadjuvant olaparib in unselected and treatment-naïve triple-negative breast cancer (TNBC) and found an objective response rate (ORR) of 56% not restricted to patients harboring germline *BRCA1/2* mutations (28). In both studies, responses to PARP inhibition were not limited to carriers of a germline *BRCA1/2*mut, making these data ideal for our Sig3 validation study.

Materials and Methods

Clinical data and patient selection

NCT01623349 is a multicenter phase Ib trial of escalating doses of olaparib and buparlisib (27). Clinical trial data were obtained from the study registered at ClinicalTrials.gov. This was a multicenter, open-label, phase Ib trial with a 3 + 3 dose-escalation design. Eligibility criteria included age of at least 18 years, diagnosis of recurrent TNBC, or diagnosis of high-grade serous ovarian cancer or recurrent breast cancer of any histology with germline *BRCA* mutations. We obtained WES and panel sequencing from 37 participants (cohort 1) based on the availability of tissue. DNA extraction and construction of libraries for massively parallel sequencing were performed as described previously (29). For the analysis of the concordance between different HRD detection methods, all 37 patients were included. For the analysis of responses, there were 5 patients who went off study in the absence of progression (radiological or clinical) and thus were not analyzed for response rates and were censored in the time-to-event analyses. The PETREMAC trial (NCT02624973) is a multicenter phase II study that included patients with stage II/III breast cancer that were stratified to eight different neoadjuvant treatment regimens. The cohort of 32 patients with TNBC (cohort 2) received initial olaparib monotherapy for up to 10 weeks, before assessment of tumor response. Clinical and radiologic evaluation of tumor size was carried out by each local investigator. Tumor biopsy studies in this report were collected before olaparib treatment and underwent targeted DNA sequencing (360 genes), as described previously (28, 30). All study participants provided written informed consent; the studies were conducted in accordance with Declaration of Helsinki ethical guidelines and approved by an institutional review board (IRB).

The Cancer Genome Atlas (TCGA) data

The germline mutation calls by TCGA were also downloaded from GDC data portal (31); the overall pathogenicity determined in that publication allowed us to select samples with germline mutations. Four samples with Prioritized VUS were not considered as germline *BRCA1/2*mut. The consensus somatic single base substitution and indel calls (32) were also downloaded from the GDC data portal (31). The samples with somatic *BRCA1/2* mutations in the TCGA BRCA and OV cohorts were selected on the basis of the presence of pathogenic annotation ClinVar database, or a damaging/deleterious effect prediction by SIFT or PolyPhen as long as these alterations were not annotated to be benign or likely benign in ClinVar.

Mutation calls

Single base substitutions

Somatic single base substitutions were calculated using MuTect2 and germline SNPs were called with HaplotypeCaller, according to the GATK best practices (33). Somatic single base substitutions with supporting read count less than 8 and 2, total depth less than 20 and 5, allelic fraction less than 0.1 and 0.05, for MSK-IMPACT panels and WES data, respectively, were filtered out.

Copy-number alterations (CNA)

Segment level CNAs were calculated using Sequenza (34) and gene-level CNAs using GISTIC (35) from the segment-level Sequenza results.

HRD detection methods

GIS calculation

Using Sequenza (34) copy-number calls and scarHRD algorithm (36), we calculated LOH [median and standard deviation (SD) in *BRCA1/2*mut tumors were 16.5 and 6.8, respectively], LST (median and SD of 25.5 and 10.3, respectively), and TAI (median and SD of 24.0 and 8.0, respectively). The sum of these quantities yields GIS. We compared the distribution of GIS values in our cohort with those from TCGA for *BRCA1/2*mut tumors (Supplementary Fig. S1). The GIS values for the TCGA were calculated from SNP arrays by the TCGA Pan-Cancer Atlas project (37, 38).

Sig3 calculation

The Sig3 calculation was carried out with SigMA algorithm (14). For analysis of TCGA tumors the in-built multivariate classifiers with *data* parameter "tcga_mc3" were used. Similarly, for MSK-IMPACT panels and WES data in cohort 1, Sig3 predictions were performed with the in-built multivariate classifiers with *data* parameter "msk" and "seqcap," respectively. The predictions were done for breast cancers and ovarian cancers separately using the corresponding tumor type settings (*tumor_type* parameter "breast" and "ovary"). For MSK-IMPACT panels, samples with less than five SNVs are classified as Sig3−. The 77% of panels in cohort 1 have ≥5 SNVs. In simulations, 91% of Sig3+ and 66% of samples have ≥5 SNVs. The samples that have <5 SNVs are accounted for in the calculation of 74% sensitivity at 10% FPR. For cohort 2, a new classifier was trained using simulations that are generated following the same procedure as described previously (14). Because of the smaller library size of panels in cohort 2 and the lower counts of SNVs, Sig3 detection was performed for all samples with ≥4 SNVs, and 75% of samples satisfied this criterion. In simulations 90% of Sig3+ and 65% of Sig3− samples have ≥4 SNVs and samples that have <4 SNVs are accounted for in the calculation of 70% sensitivity at 10% FPR. In this study, we used the threshold in WES data that corresponds to 5% FPR and 90% sensitivity, and the one that corresponds to 10% FPR and 75% sensitivity in panel data to define Sig3+ tumors. The sensitivity and FPR are determined using panel and WES simulations generated by down-sampling WGS data with respect to the ground truth defined on the basis of the Sig3 calculation in WGS data.

SigProfiler calculation

To compare SigMA-based Sig3 calculation to other popular signature analysis methods, we used SigProfiler (39). The *de novo* signature analysis with SigProfiler found 3 signatures in our cohort. The signatures were matched to the COSMIC catalog v3 and those with the highest cosine similarity were identified. Signature A was most similar to Sig3 (Supplementary Fig. S2).

Sig3 selection thresholds for SigMA

To define Sig3+ samples from panel and WES data, we used thresholds that correspond to 10% and 5% FPR, respectively. The 10% FPR threshold was found to capture more true positives and had an overall better predictive value of response, whereas in WES data the 5% threshold selects samples with higher Sig3 exposure (Supplementary Fig. S3) and allows better separation in PFS. These results are summarized in:

- Comparison of GIS and Sig3 exposures in WES data between samples that have SigMA scores above the 5% and 10% FPR thresholds (Supplementary Fig. S3).
- Comparison of PFS between Sig3+ and Sig3− samples with different thresholds. In panel data, the PFS was also better associated with the 10% FPR (reported in Results section) compared with 5% FPR ($P = 0.57$; median 5.7 and 7.7). Instead, in WES data, the 10% threshold provided worse PFS separation ($P = 0.19$; median 5.63 and 6.97) compared with 5% threshold (reported in the Results section).
- The number of patients that are *BRCA1/2*mut in different Sig3 categories (Supplementary Fig. S4).

Comparison of Sig3 detection with SigMA in WES data compared with other methods

The detection of Sig3 from WES with SigMA and 5% FPR threshold compared with alternative signature detection approaches. We compared PFS of WES-Sig3+ classification with SigMA to PFS of samples with positive Sig3 exposure calculated by NNLS (Supplementary Fig. S5) as well as with nonnegative matrix factorization (NMF; as implemented in SigProfiler algorithm; Supplementary Fig. S2). A significantly longer PFS is observed in samples that had a Signature A exposure greater than 25, but the association was still inferior in comparison with SigMA classification (lower significance, smaller PFS increase 2.2 months vs. 4.24 months with SigProfiler and SigMA, respectively). Confirming our observation of lower Sig3 exposure in Sig3− samples with NNLS, the NMF analysis yielded a similarly low exposure distribution in the WES-Sig3− group (Supplementary Fig. S2) even if there were samples with positive exposures. The Sig3+ samples selected with SigMA associate better to the PFS compared with other signature analysis methods.

Survival analysis

Survival analyses were performed with the Kaplan–Meier method using survival R package. Patients stratified according to Sig3 status and tumor type. Curves were compared using the log-rank method. A Cox regression analysis was performed to estimate the effect size of each feature. The *P* values for Cox-regression were calculated by Wald test.

Pathway analysis

The difference in copy-number gain and loss frequencies of genes is used to calculate geneset enrichment scores with ReactomePA package (Supplementary Table S1). The gene level differences can be found in Supplementary Table S2.

Code availability

The SigMA algorithm is available on GitHub (https://github.com/parklab/SigMA). The code used in the analysis will be provided upon request from the authors.

Data availability

The authors support the dissemination of research data that has been generated, and increased cooperation between investigators. The data that support the findings of this study are available at doi:10.17632/zg5xvm3f3w.1. Raw data for this study were generated at the Dana-Farber Cancer Center and Memorial Sloan Kettering Cancer Center. Derived data supporting the findings of this study are available at the database of Genotypes and Phenotypes (dbGaP) via study accession: phs003019.v1.p1. Further de-identified individual participant data will be provided according to institutional procedures. Requests addressed to G.M. Wulf must include a description of the nature of the proposed research and extent of data requirements. Data recipients are required to enter a formal data sharing agreement that describes the conditions for release and requirements for data transfer, storage, archiving, publication, and intellectual property. Requests are reviewed by the study team in terms of scientific merit and ethical considerations, including patient consent.

Haukeland University Hospital and the University of Bergen support the dissemination of research data and cooperation between investigators nationally and internationally. On the basis of current Norwegian laws and regulations, and the biobank approval for the PETREMAC trial given by the Regional Ethics Committee Western Norway before the study commenced, genomic data are not to be made openly available. After publication and upon formal request, raw sequencing data, including de-identified individual participant data and a data dictionary defining each field in the data set, may be shared according to institutional guidelines, pending project-specific approvals from the Regional Ethics Committee in Norway. Requests are via a standard pro forma describing the nature of the proposed research and extent of data requirements. Data recipients are required to enter a formal data sharing agreement that describes the conditions for release and requirements for data transfer, storage, archiving, publication, and intellectual property. Requests are reviewed by the PETREMAC study team in terms of scientific merit and ethical considerations, including patient consent. An evaluation as described above will typically take three months. Requests may be directed to H. P. Eikesdal.

Results

Cohorts and high-throughput sequencing

NCT01623349 was a multicenter phase Ib trial of escalating doses of olaparib and buparlisib (27). Archival tumor material was collected prior to enrollment, and WES, and panel sequencing was obtained from the 37 patients (cohort 1) based on the availability of tissue. These patients include 26 with high-grade serous ovarian cancer (including four fallopian tube and two primary peritoneal tumors) and 11 with TNBC (**Fig. 1A**). Panel sequencing was performed using the MSK-IMPACT (Memorial Sloan Kettering-Integrated Mutation Profiling of Actionable Cancer Targets) panel, which covers 341 genes (2.1 Mb). WES was performed using solution hybrid selection (73.7 Mb). We determined the Sig3 status from both panel and WES data using SigMA. We also calculated the GIS from WES data with the scarHRD algorithm (36). We compared the GIS in *BRCA1/2* mutant tumors in our cohort to the calculation by the PanCanAtlas consortium in the TCGA data. (See Materials and Methods for detailed information.) The PETREMAC study was a phase II trial evaluating olaparib monotherapy in the neoadjuvant setting for 32 patients with untreated TNBC (cohort 2; ref. 28). Pre-treatment biopsies were extracted and submitted for targeted DNA sequencing applying a 360-gene panel (1.5 Mb; ref. 30). Cohort 1 had on average 9.9 mutations (median = 7; SD = 9.5) per sample and cohort 2 had 6.96 (median = 5; SD = 5.0) mutations. It is important to note that using synonymous and noncoding region mutations increases the counts of mutations available for signature analysis and improves the detection accuracy. The 77% and 57% of mutations used in the signature analysis for cohorts 1 and 2 were either noncoding or synonymous.

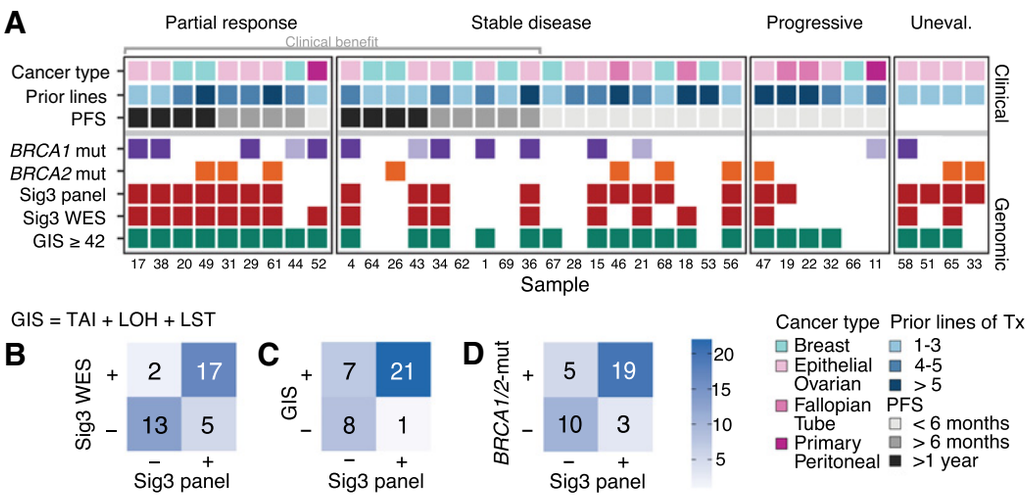

Figure 1.

Cohort 1 details and comparison of different HRD detection methods. **A,** Clinical and genomic characteristics for each sample (small numbers at the bottom represent the individual study ID of each participant), grouping based on RECIST best overall response criteria. Clinical characteristics include the different cancer types and number of prior treatments. Different intervals of PFS are shown in the third row. Genomic characteristics include *BRCA1/2* mutation status, Sig3+ classification by SigMA from panel and WES data, and the GIS calculated from WES. The lighter fill color of *BRCA1/2*mut indicates lack of LOH. **B,** 2 × 2 table of Sig3 status identified from WES and panel concordance is 81%. **C,** 2 × 2 table of GIS calculated with scarHRD versus Sig3 status from panel data. **D,** Mutations of *BRCA1/2* versus Sig3 status. One patient had both a *BRCA1* and *BRCA2* mutation. Tx, therapy; WT, wild type.

Sig3 predictions with SigMA algorithm

The SigMA algorithm infers the HRD status from panel data by estimating the likelihood that the observed mutational spectrum results from Sig3 (14). A compendium of WGS cases collected by the International Cancer Genome Consortium (ICGC) provides the resource for determining which signatures tend to co-occur and their frequencies in different tumor tissue types (40). The likelihood measure indicates the compatibility of mutations identified in a patient to the expected mutational spectra of Sig3+ tumors in the ICGC data. By combining these likelihoods with other signature-related features in a multivariate machine-learning classifier, SigMA robustly predicts the presence of mutations from Sig3. Classifiers are trained using realistic simulations of panels or WES obtained by down-sampling whole genomes (WGS) that provide the "true" Sig3 tags. The sensitivity and false-positive rate (FPR) are calculated by comparing the Sig3 classification in simulated panels or WES to the categories in WGS data. For MSK-IMPACT panels used to sequence cohort 1, Sig3 detection was shown to have a sensitivity of 74% at 10% FPR (14). In cohort 1, the previously described (14) classifiers and thresholds (<5% and <10% FPR) were employed directly without any retraining for Sig3 classification from panels and WES. For cohort2, following the procedure described above, we simulated panels according to the specific library coverage and used the simulations to train a new classifier yielding a sensitivity of 70% at 10% FPR. For panel data in cohorts 1 and 2, we defined samples with a SigMA score larger than that corresponding to 10% FPR as Sig3. We adopted a more stringent selection criterion corresponding to a <5% FPR to define Sig3+ tumors in WES. Higher counts of mutations in WES compared with panels allow a reduction in FPR without leading to a dramatic decrease in sensitivity (see Materials and Methods for more information).

Validation of sig3 predictions from panels using exomes

The Sig3 classification was in agreement between WES and panel data for 30 of 37 patients (81% concordance). For the remaining 7 patients, 5 tested Sig3+ only for their panel data, and 2 tested Sig3+ only for their WES data (**Fig. 1B**). More stringent selection criterion in WES data preferentially selects samples with a higher burden of Sig3, and the Sig3− category may include tumors with a nonnegligible but low burden of Sig3, partly explaining why there are more panel-Sig3+/WES-Sig3− samples compared with panel-Sig3−/WES-Sig3+ cases (Materials and Methods; Supplementary Figs. S1 and S2).

HRD predictions using sig3 from panel and GIS have a significant overlap

We then compared the level of concordance with GIS for panel-Sig3 and WES-Sig3. For GIS, we imposed a threshold of 42 to define HRD based on prior work (7). As shown in **Fig. 1C**, between panel-Sig3 and GIS, there was an agreement for 29 of 37 cases (78% concordance); between WES-Sig3 and GIS, there was an agreement for 28 of 37 samples (76% concordance). These suggest that panel-Sig3 provides an adequate proxy for WES-Sig3 in comparing substitution-based signature with genome instability as measured by GIS. There are seven cases with GIS+ / panel-Sig3−, but five of these were also WES-Sig3−, suggesting that the difference is between substitution-based versus CNV-based signature, rather than a panel versus exome difference. Two tumors were GIS− / panel-Sig3+ / WES-Sig3−, potentially indicating a false positive HRD assignment from panel sequencing. In addition, four out of seven with GIS+ / Sig3− (panel) had borderline GIS values. Although a very good correlation has been reported between WES and SNP-array dependent GIS values (36), minor adjustments may be necessary for selecting the optimal threshold. A higher threshold of GIS ≥49 provided the highest concordance of 86% with panel-Sig3 and 84% with WES-Sig3 (Supplementary Fig. S3).

Overall, the high concordance between Sig3 calls from panel and exomes as well as between GIS score and Sig3 positivity provides orthogonal validation that panel-Sig3 can be used to identify HRD tumors. The HRD tumors defined by Sig3-positivity have a higher response rate to PARPi. The small number of discordant cases between Sig3 and GIS may reflect either the differences in the accuracies of the methods in identifying HRD, differences in underlying mechanisms that cause copy-number variations and single-base substitutions in HRD tumors, or a combination of both. The impact of these different HRD biomarkers on clinical outcomes following treatment with PARPi is discussed in a later section.

Sig3 and GIS detect HRD in most BRCA1/2mut tumors

Cohort 1 had 24 *BRCA1/2*mut tumors of germline origin with 14 *BRCA1*mut and 10 *BRCA2*mut cases (**Fig. 1A**). As shown in **Fig. 1D**, there was a significant association of *BRCA1* or *BRCA2* mutations ($P = 0.0049$, Fisher exact test) with Sig3 positivity; 79% (19/24) of *BRCA1/2*mut were panel-Sig3+, 71% (17/24) were WES-Sig3+, and 87% (21/24) were GIS+. Five patients—4 *BRCA1*mut and 1 *BRCA2*mut—had panel-Sig3−, and 4 of these patients were also WES-Sig3−, indicating that a fraction of *BRCA1/2*mut cancers arises through mechanisms unrelated to the development of Sig3. These Sig3− *BRCA1/2*mut samples also exhibited a numerically lower GIS than Sig3+ *BRCA1/2*mut cases (Supplementary Fig. S3). Among the *BRCA1/2* WT samples, 23% (3/13) were identified as panel-Sig3+. For 6 of the 24 *BRCA* mutations, the pathogenicity of the mutation according to ClinVar was uncertain ($n = 2$), or LOH of the second *BRCA1/2* allele with a copy-number loss or somatic mutations could not be established ($n = 4$). The two samples with *BRCA1/2* alterations that qualify as variants of uncertain significance (VUS) were also Sig3+, supporting their classification as HRD positive. Two of the four samples without biallelic loss were Sig3+, and the remaining two samples were Sig3−. Overall, we find that 20/24 (83%) *BRCA1/2*mut patients had a biallelic loss, mostly due to LOH.

It is important to highlight that the response rate among *BRCA1/2*mut tumors to PARPi therapy is approximately 50%. Thus, discordance—or imperfect overlap—between these HRD detection approaches and *BRCA1/2* mutations does not necessarily suggest weakness of the method. Instead, it may indicate the potential for further refinement of patient selection. Hence, comparing different methods in terms of patient outcomes is a critical step in assessing these biomarkers.

Sig3+ predicts longer PFS better than GIS+ and BRCA1/2mut in ovarian or breast cancer treated with PARPi

We evaluated the relationship of Sig3 positivity with PFS in this cohort of 37 patients with advanced and heavily pretreated ovarian cancer ($n = 26$) and TNBC ($n = 11$) who were uniformly treated with a PARPi-containing regimen in a clinical trial setting (see Materials and Methods for details; ref. 27). PFS was significantly longer (log-rank test; $P = 0.036$) in the panel-Sig3+ group, with a median of 7.7 months, compared with the Sig3− group, with a median of 5.6 months (**Fig. 2A**). Similarly, median PFS in the Sig3+ group identified with SigMA on WES data was 8.5 compared with 5.0 in the Sig3− group, (log-rank test; $P = 0.0057$; **Fig. 2B**).

Although Sig3+ (WES or panel) was associated with a significantly longer PFS, GIS and *BRCA1/2*mut were not observed to have any association with PFS (log-rank test: $P = 0.37$ and 0.10,

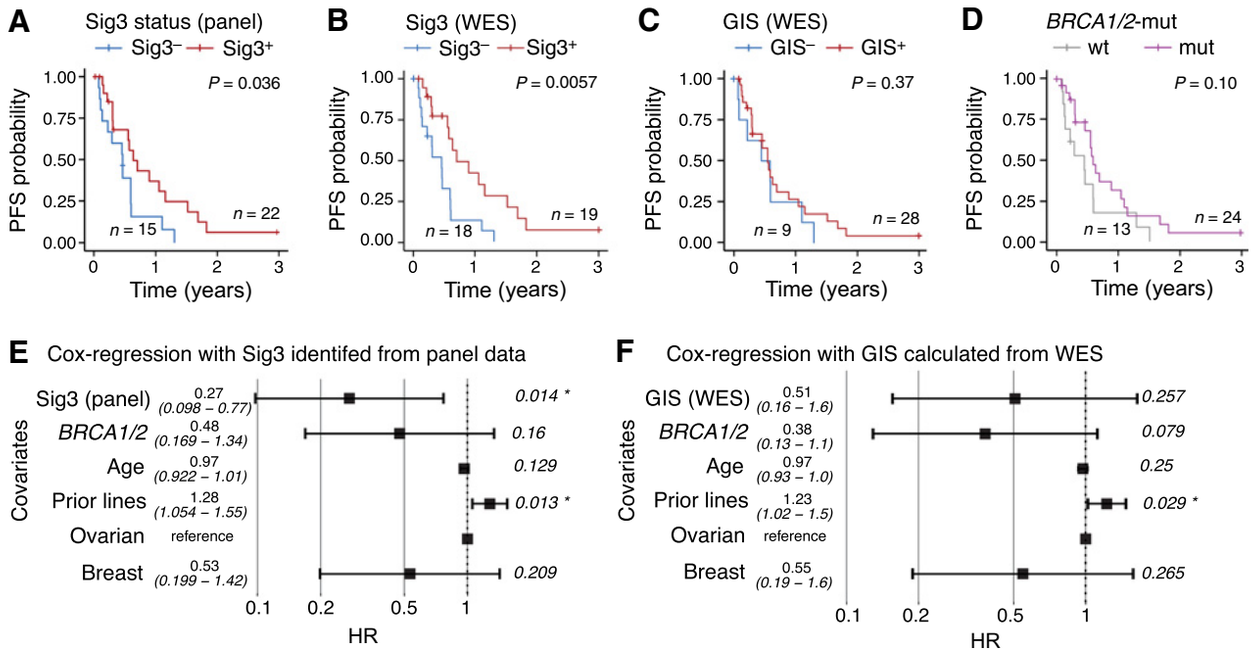

Figure 2.

Survival analysis according to (**A** and **B**) Sig3 status using panel data (median survival: 5.6 vs. 7.7 months in Sig3− and Sig3+ samples, respectively) and WES (median survival: 5.0 vs. 8.5 in Sig3− and Sig3+ samples respectively); **C,** GIS (median survival: 5.6 months vs. 7.0 months in GIS+ and GIS− samples, respectively); **D,** *BRCA1/2*mut or WT (median survival: 5.5 months vs. 7.3 months in WT vs. *BRCA1/2*mut samples, respectively). Cox multivariate regression including (**E**) Sig3 status or (**F**) GIS. Age, ECOG, and stage as covariates did not have significant HR and were not included as covariates. "Prior lines" refers to the number of previous lines of therapy in the metastatic setting.

respectively; **Fig. 2C** and **D**). The GIS+ / panel-Sig3− patients had a short PFS, similar to the GIS− / panel-Sig3− cases (Supplementary Fig. S5). The selection with GIS ≥ 49 was somewhat better in predicting PFS than the GIS ≥ 42 selection but did not change the general conclusion (Supplementary Fig. S1). Accounting for potential confounding factors such as prior lines of treatment, age, and cancer type in the Cox regression analysis decreased HRs of progression or death for *BRCA1/2*mut and patients with GIS ≥ 49, although Sig3 panel or WES remained the most promising biomarker with the lowest hazard ratio and tighter confidence intervals (Supplementary Figs. S1 and S6). Loss-of-function mutations in other genes potentially associated with homologous recombination that could explain the response to PARPi were not identified.

When combined in a Cox regression model, Sig3 status was significant ($P = 0.03$; HR, 0.34; **Fig. 2E**) and *BRCA*1/2 status was not ($P = 0.26$). This combined analysis shows that Sig3 brings additional information that allows better stratification of HRD patients beyond *BRCA1/2*mut status. These findings suggest that there is a great deal of heterogeneity in PFS among the *BRCA1/2*mut cases and that *BRCA1/2*mut status is less informative than the Sig3 status. When GIS is used in place of Sig3, it was not statistically significant ($P = 0.40$ and 0.069 for 42 and 49 thresholds, respectively: **Fig. 2F**; Supplementary Fig. S1E). The number of previous lines of therapy was significantly associated with a higher risk of progression ($P = 0.003$; HR, 4.24 in the Sig3 model and $P = 0.006$; HR, 3.49 in the GIS model; **Fig. 2E** and **F**), likely related to the acquisition of cross-resistance between platinum and other DNA damaging chemotherapies and PARPi. These results suggest that panel-Sig3 may serve as a biomarker to identify HRD cancers most likely to respond to PARPi independently of previous therapy.

PARPi have been approved for *BRCA1/2* carriers in various cancer types. Therefore, an immediate step towards more comprehensive HRD detection would be to include patients based on their *BRCA1/2*mut as well as Sig3 status to identify a larger number of patients potentially responding to PARP inhibition. A similar approach has been adopted for GIS-based commercial tests. In later stages, it may be possible to explore the use of Sig3 to increase the specificity of HRD detection by differentiating between *BRCA1/2*mut tumors with and without HRD. Our current analysis does not allow a definitive conclusion in this respect. Defining panel-Sig3+ and/or *BRCA1/2*mut patients as HRD, we find a significantly higher response rate (per RECIST, version 1.1 criteria) to PARPi in HRD patients (9/23: 39%) compared with non-HRD patients (0/10, 0%; Fisher exact test; $P = 0.03$).

ATR amplification confers resistance to PARPi

To identify additional genetic factors that may impact PFS, we examined the association of CNAs of single genes implicated in HRD with PFS. We focused on the role of CNAs of *ATR*, *TP53BP1*, *EZH2*, and *POLQ*, as these genes have been implicated in PARPi resistance through replication fork stabilization (41). Among these, *ATR* amplification was significantly associated with shorter PFS (log-rank test: $P = 0.01$; **Fig. 3A**). Although other CNAs also had a trend towards shorter PFS, they were not statistically significant (Supplementary Fig. S7). Upon inclusion into the Cox regression model, *ATR* amplification is associated with worse PFS with a hazard ratio of 4.48, whereas HRD is associated with better PFS with a HR of 0.16 (**Fig. 3B**). When samples are stratified according to HRD and *ATR* amplification into four groups, the longest PFS is obtained for Sig3+ patients without

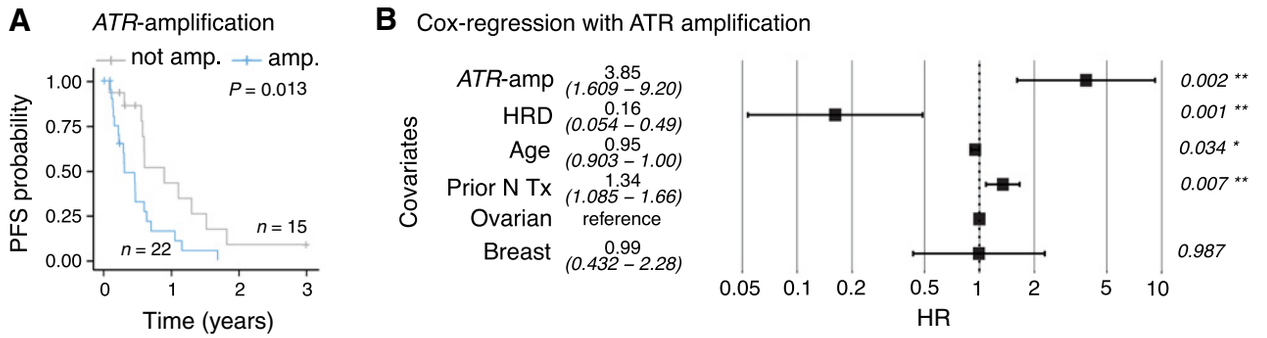

Figure 3.

Survival analysis according to (**A**) *ATR* amplification (median PFS 5.0 months vs.10.9 months, respectively, for samples with *ATR* amplification and those without). **B,** Cox model same as in **Fig. 2E** but with the additional covariate of *ATR* amplification. HRD is defined as panel-Sig3+ and/or *BRCA1/2*mut. "Prior N Tx" refers to number of prior lines of therapy.

ATR amplification (Supplementary Fig. S7). Notably, 7 patients with HRD tumors did not have clinical benefit—defined as a radiologic response or stable disease for at least 6 months—from the treatment. Five of these seven tumors were found to have *ATR* amplification, possibly explaining the lack of response. These exploratory and hypothesis-generating results suggest that adding *ATR* amplification status to Sig3 may be informative although the determination as to whether *ATR* amplification is associated with primary or acquired resistance will require analysis of larger datasets of tumors from patients treated with PARPis.

External clinical validation of panel-Sig3 in TNBC using data from the phase II PETREMAC trial

Cohort 2 (from the PETREMAC trial) and the study results were previously described in detail (28). In brief, the phase II PETREMAC trial included patients with primary TNBC >2 cm, and patients received olaparib for up to 10 weeks before response assessment. The calculation of panel-Sig3 using targeted DNA sequencing (360 genes) from tumor biopsies collected before olaparib (treatment-naïve tumors) revealed that most tumors (59%) are classified as Sig3+ (**Fig. 4A**). For comparison, the frequency of Sig3+ tumors in TCGA (**Fig. 4B**). Of the 19 patients classified as panel-Sig3+, only 4 patients were carriers of a germline *BRCA1/2* mutation (**Fig. 4C**), underscoring that Sig3 identifies patients with HRD beyond g*BRCA1/2* mutations. We compared the ORR of patients classified as panel-Sig3+ with patients classified as panel-Sig3− and found that the ORR in the former group is higher than in the latter (74% vs. 31%, $P = 0.029$; **Fig. 4D**).

Analysis of TCGA data identifies many Sig3+ breast and ovarian cancers beyond BRCA carriers

Cohort 1 is enriched for *BRCA1/2*mut patients as opposed to an unbiased selection of TNBCs and HGSOCs. To provide estimates on the frequency of Sig3+ tumors in a patient population not enriched for

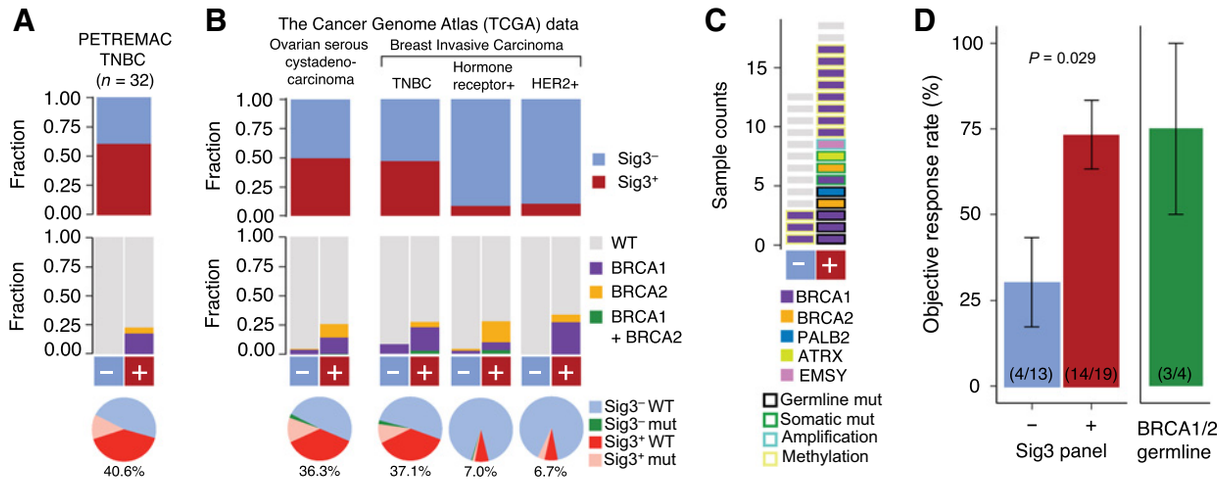

Figure 4.

Fraction of samples that are Sig3+ (top), the proportion of samples with germline *BRCA1/2*mut for Sig3+ and Sig3− groups (middle), and pie charts showing the fraction of samples that are Sig3+ germline *BRCA1/2* WT in TNBCs from PETREMAC trial (**A**) and TCGA ovarian cancers and the major clinical subtypes of breast cancer (**B**). The fraction of samples that are Sig3+ but not germline *BRCA1/2*mut are shown below the pie charts in red and the fractions are indicated below. Pink: Sig3+ and germline *BRCA1/2*mut, Green: Sig3− and germline *BRCA1/2*mut, and Blue Sig3− and germline *BRCA1/2* WT. **C,** HR-gene alterations in patients from the PETREMAC trial. **D,** ORR from patients from the PETREMAC trial according to panel-Sig3 classification and etiology of Sig3. Error bars denote the SE. The number of samples and the responders are denoted in parenthesis. WT, wild type.

tumors with deleterious *BRCA1/2* mutation, we analyzed WES data from 901 unselected breast cancer samples and 454 unselected ovarian serous cystadenocarcinomas samples from TCGA. We found that 47% and 50% of TNBC and ovarian cancers can be classified as Sig3+ whereas only 11% and 14% have a germline *BRCA1/2* mutation, respectively (**Fig. 4B**). Somatic *BRCA1/2* mutations were found in only a minority of these tumors and constituted 8% and 5% of TNBCs and ovarian cancers, respectively. If we focus on TNBC, where the indication for PARPi is currently limited to carriers of a germline *BRCA* mutation, Sig3 could identify an additional 37% of patients who might be candidates for PARPi. Even though at a lower rate, hormone receptor or HER2-positive breast cancer were also classified as Sig3+ and hence these patients could potentially benefit from HRD-targeted therapy (i.e., PARPi). Thus, Sig3-based detection has the potential to substantially increase the number of patients who benefit from PARPi beyond those with germline *BRCA1/2* mutations.

Discussion

In this study, we show that the Sig3 classification from clinical panel sequencing could potentially serve as a surrogate for Sig3 from exomes and, more importantly, is predictive of response to a PARPi combination, surpassing the predictive value of either *BRCA1/2* status or GIS. We provide the first analytical validation that the Sig3 classification from gene panels has excellent concordance with that derived from WES data from patients with breast and ovarian cancers (cohort 1). This study also provides clinical validation of panel-Sig3 as a predictive biomarker in patients with breast and ovarian cancer receiving combined olaparib/buparlisib (cohort 1). In addition, for the first time, we clinically validate panel-Sig3 as predictive of olaparib response in a population with treatment-naïve and unselected TNBC (cohort 2). This means that the SigMA algorithm can be applied to panel sequencing data currently obtained for patients as part of their routine care for metastatic solid tumors, and thus, is an immediately available resource to contribute to HRD prediction. Although panel sequencing is currently standard-of-care for most metastatic cancers to pinpoint therapeutic targets, the implementation of Sig3 calculation adds minimal compute cost and time. This contrasts with other methods such as GIS, which requires WES, or an additional commercial assay, or HRDetect, which requires WGS from fresh biopsies. Hence, Sig3 status extracted from panel sequencing commonly used in the clinic, has the potential to aid decision-making on the use of PARP inhibitors, and should be added as an exploratory biomarker in ongoing studies and as an integral marker in future clinical trials. It is important to note that all patients with partial response tested positive for Sig3 or a *BRCA1/2* mutation, whereas three patients derived a clinical benefit who were neither Sig3 positive nor carried a *BRCA1/2* mutation, implying that we still lack the tools to identify all patients who benefit from PARP inhibition, or that PARPi may have mechanisms of action independent of HRD. In cohort 1, 2 patients were panel-Sig3+ but did not carry a *BRCA1/2* mutation, and 1 of these patients had a partial response and PFS longer than 1 year with the PARP–PI3K inhibitor combination. Biologically, this finding raises the possibility that HRD is a polygenic phenotype that is only captured by a genomic signature rather than single mutational driver events in some tumors. If a patient's tumor was panel-Sig3+ or *BRCA1/2*m, the ORR was 39% and the clinical benefit rate was 65%. If neither was present, the ORR was 0%, and the clinical benefit rate was 30%. In cohort 2, the ORR was 74% for patients whose tumor was panel-Sig3+ or *BRCA1/2*m, whereas the group of patients with panel-Sig3− tumors had a significantly lower ORR of 31%.

It is noteworthy that in cohort 1, all patients who achieved an objective response tested positive for either Sig3 or *BRCA1/2*. Among patients who had progressive disease as their best response (primary resistance), there were two *BRCA1/2*mut patients, one of whom was Sig3+, but the patient had more than seven prior lines of treatment. Whether the absence of Sig3 can be used to predict primary resistance to PARP inhibition among *BRCA1/2* carriers is unclear at this point. The overall response rate to olaparib in germline *BRCA1/2* mutation carriers with metastatic breast cancer is 59.9%, that is, 40% of patients experience primary resistance (2), the mechanism of which is poorly understood. Secondary, acquired resistance to PARPi can occur through the reversal of HR gene mutations, restoration of HR through end-resection, or replication fork stabilization (42). These secondary resistance mechanisms are thought to be facilitated by the high evolutionary plasticity of HRD tumors, resulting in frequent CNAs that may lead to the recovery of some HR function during PARPi therapy. Observed secondary resistance mechanisms are the amplification of the *ATR* gene leading to upregulation of the ATR/CHK1 pathway improving fork stability (43) or loss of *TP53BP1* which partially restores HR (44). In cohort 1, we did find that ATR amplification was associated with shorter PFS. Ultimately, Sig3+ may be an indicator of the underlying HRD, but the clinical response to PARPi will also depend on the presence of mechanisms of resistance that are not captured with this signature.

Limitations of our study include the small numbers of patients in both cohorts, which limits our ability to explore the subgroups further, and the combination treatment in cohort 1. In addition, we were only able to analyze pretreatment tumor tissue samples and no on- or posttreatment tissues were available to examine changes induced by PARP inhibition. Among the 37 patients from cohort 1, there were only 13 patients who were *BRCA1/2* WT, likely from ascertainment bias at enrollment favoring the enrollment of patients with *BRCA1/2*mut into a PARPi trial. Of note, BKM-120 was not considered to be efficacious at the studied doses as the MTD was only 60 mg/day, well below what was considered meaningful PI3K inhibition based on pharmacokinetics and pharmacodynamics data (27). Therefore, we consider the responses seen in our cohort as mostly driven by olaparib, which was dosed at 200 mg twice a day in this study, a dose that to date would be considered below standard of care.

In summary, patients with Sig3+ tumors are more likely to respond to PARPi and have longer PFS. The implementation of Sig3 analysis with SigMA could be applied to clinical sequencing data without a considerable increase in cost and time. Prospective validation of the clinical utility is warranted in the setting of a biomarker-driven clinical trial.

Authors' Disclosures

F. Batalini reports personal fees from Curio Science outside the submitted work. N. M. Tung reports personal fees and other support from AstraZeneca during the conduct of the study. E.P. Winer reports other support from Carrick Therapeutics, Genentech/Roche, Genomic Health, GSK, Jounce, and Leap Therapeutics outside the submitted work. E.L. Mayer reports other support from AstraZeneca during the conduct of the study, as well as other support from Novartis, Gilead, and Lilly outside the submitted work. S. Knappskog reports grants and personal fees from AstraZeneca, grants from Pfizer and Illumina, and personal fees from Pierre Fabre outside the submitted work. P.E. Lønning reports grants from AstraZeneca during the conduct of the study; P.E. Lønning also reports grants from Novartis, Pfizer, and Illumina, as well as personal fees from AstraZeneca, Pierre Fabre, Roche, AbbVie, Akamedikonferens, AstraZeneca, and Laboratorios Farmaceuticos Rovi outside the submitted work. In addition, P.E. Lønning reports ownership of Cytovation Ltd. stock. U.A. Matulonis reports personal fees from AstraZeneca, GSK, Merck, and Novartis during the conduct of the study, as well as personal fees from Trillium, Boehringer Ingelheim, Immunogen, Next Cure, 2X Oncology, Agenus, and Blueprint Medicines outside the submitted work. D.B. Solit reports personal fees from Pfizer, Loxo/Lilly Oncology,

Vividion Therapeutics, BridgeBio, Scorpion Therapeutics, FORE Therapeutics, and Fog Pharma outside the submitted work. H.P. Eikesdal reports grants and nonfinancial support from AstraZeneca, as well as personal fees from AstraZeneca and Pfizer during the conduct of the study; H.P. Eikesdal also reports personal fees from Novartis, Amgen, HAI Interaktiv, Bristol Myers Squibb, Dagens Medisin, Eli Lilly, Gilead Sciences, Pfizer, Pierre Fabre, Roche, Aptitude Health, Daiichi Sankyo, MSD, Sanofi Aventis, Seagen, Adelphi Targis, and AstraZeneca outside the submitted work. P.J. Park reports a patent for SigMA software pending, licensed, and with royalties paid from Pfizer. G.M. Wulf reports grants from Breast Cancer Research Foundation, Breast Cancer Alliance, May Kay Ash Foundation, Ovarian Cancer Research Foundation, NIH R01 CA 226776, P50 CA 168504, and SU2C-AACR-DT0209 during the conduct of the study, as well as other support from GlaxoSmithKline outside the submitted work; G.M. Wulf also has a patent for compositions and methods for the treatment of proliferative diseases pending. No disclosures were reported by the other authors.

Authors' Contributions

F. Batalini: Conceptualization, resources, data curation, formal analysis, supervision, validation, investigation, visualization, methodology, writing–original draft, project administration, writing–review and editing. **D.C. Gulhan:** Conceptualization, resources, data curation, software, formal analysis, supervision, validation, investigation, visualization, methodology, writing–original draft, project administration, writing–review and editing. **V. Mao:** Data curation, software, formal analysis, investigation, visualization, methodology. **A. Tran:** Data curation, software, formal analysis, investigation, visualization, methodology. **M. Polak:** Project administration. **N. Xiong:** Writing–review and editing. **N. Tayob:** Writing–review and editing. **N.M. Tung:** Conceptualization, resources, supervision, writing–review and editing. **E.P. Winer:** Resources, writing–review and editing. **E.L. Mayer:** Resources, writing–review and editing. **S. Knappskog:** Resources, data curation, investigation, writing–review and editing. **P.E. Lønning:** Resources, writing–review and editing. **U.A. Matulonis:** Resources, writing–review and editing. **P.A. Konstantinopoulos:** Resources, writing–review and editing. **D.B. Solit:** Resources, funding acquisition, writing–review and editing. **H. Won:** Resources, formal analysis, investigation, writing–review and editing. **H.P. Eikesdal:** Conceptualization, resources, investigation, writing–review and editing. **P.J. Park:** Conceptualization, resources, data curation, software, formal analysis, supervision, funding acquisition, validation, investigation, visualization, methodology, writing–original draft, project administration, writing–review and editing. **G.M. Wulf:** Conceptualization, resources, data curation, supervision, funding acquisition, validation, investigation, visualization, methodology, writing–original draft, project administration, writing–review and editing.

Acknowledgments

D.C. Gulhan, G.M. Wulf, and P.J. Park were supported by the Harvard Ludwig Center. Institutional funding was provided to H.P. Eikesdal, S. Knappskog, and P.E. Lønning by The KG Jebsen Foundation (SKGJ-MED-020), AstraZeneca (ESR-14-10077), and Pfizer (GMGS #51752519). H.P. Eikesdal was supported by Helse Vest Regionalt Helseføretak (#912252). S. Knappskog was supported by the Norwegian Cancer Society (Kreftforeningen; 190281-2017). P.E. Lønning was supported by the Norwegian Research Council (273354), Helse Vest Regionalt Helseføretak (912008), and the Norwegian Cancer Society (190275-2017). G.M. Wulf was supported by a Stand Up to Cancer–American Association for Cancer Research Dream Team Translational Cancer Research Grant SU2C-AACR-DT0209, and a National Institutes of Health (NIH) Research Project Grant 1R01CA226776-01. E.P. Winer, G.M. Wulf, and E.L. Mayer are supported by the DF/HCC Specialized Program of Research Excellence (SPORE) in Breast Cancer, NIH Grant P50 CA168504. U.A. Matulonis is funded by the NCI P50 CA240243-01A1 and the Breast Cancer Research Foundation. G.M. Wulf reports grants from Mary Kay Ash Foundation, Ovarian Cancer Research Foundation, Breast Cancer Alliance, and Breast Cancer Research Foundation.

The publication costs of this article were defrayed in part by the payment of publication fees. Therefore, and solely to indicate this fact, this article is hereby marked "advertisement" in accordance with 18 USC section 1734.

Note

Supplementary data for this article are available at Clinical Cancer Research Online (http://clincancerres.aacrjournals.org/).

Received March 8, 2022; revised May 5, 2022; accepted August 29, 2022; published first September 1, 2022.

References

1. Mirza MR, Monk BJ, Herrstedt J, Oza AM, Mahner S, Redondo A, et al. Niraparib maintenance therapy in platinum-sensitive, recurrent ovarian cancer. N Engl J Med 2016;375:2154–64.
2. Robson M, Im S-A, Senkus E, Xu B, Domchek SM, Masuda N, et al. Olaparib for metastatic breast cancer in patients with a germline BRCA mutation. N Engl J Med 2017;377:523–33.
3. Golan T, Hammel P, Reni M, Van Cutsem E, Macarulla T, Hall MJ, et al. Maintenance olaparib for germline BRCA-mutated metastatic pancreatic cancer. N Engl J Med 2019;381:317–27.
4. González-Martín A, Pothuri B, Vergote I, DePont Christensen R, Graybill W, Mirza MR, et al. Niraparib in patients with newly diagnosed advanced ovarian cancer. N Engl J Med 2019;381:2391–402.
5. de Bono J, Mateo J, Fizazi K, Saad F, Shore N, Sandhu S, et al. Olaparib for metastatic castration-resistant prostate cancer. N Engl J Med 2020;382:2091–102.
6. Tung NM, Robson ME, Ventz S, Santa-Maria CA, Marcom PK, Nanda R, et al. TBCRC 048: a phase II study of olaparib monotherapy in metastatic breast cancer patients with germline or somatic mutations in DNA damage response (DDR) pathway genes (Olaparib Expanded). JCO 2020;38:1002.
7. Alexandrov LB, Nik-Zainal S, Wedge DC, Aparicio SAJR, Behjati S, Biankin AV, et al. Signatures of mutational processes in human cancer. Nature 2013;500:415–21.
8. Alexandrov LB, Kim J, Haradhvala NJ, Huang MN, Tian Ng AW, Wu Y, et al. The repertoire of mutational signatures in human cancer. Nature 2020;578:94–101.
9. Nik-Zainal S, Davies H, Staaf J, Ramakrishna M, Glodzik D, Zou X, et al. Landscape of somatic mutations in 560 breast cancer whole-genome sequences. Nature 2016;534:47–54.
10. Polak P, Kim J, Braunstein LZ, Karlic R, Haradhavala NJ, Tiao G, et al. A mutational signature reveals alterations underlying deficient homologous recombination repair in breast cancer. Nat Genet 2017;49:1476–86.
11. Davies H, Glodzik D, Morganella S, Yates LR, Staaf J, Zou X, et al. HRDetect is a predictor of BRCA1 and BRCA2 deficiency based on mutational signatures. Nat Med 2017;23:517–25.
12. Timms KM, Abkevich V, Hughes E, Neff C, Reid J, Morris B, et al. Association of BRCA1/2 defects with genomic scores predictive of DNA damage repair deficiency among breast cancer subtypes. Breast Cancer Res 2014;16:475.
13. Hoppe MM, Sundar R, Tan DSP, Jeyasekharan AD. Biomarkers for homologous recombination deficiency in cancer. J Natl Cancer Inst 2018;110:704–13.
14. Gulhan DC, Lee JJ-K, Melloni GEM, Cortés-Ciriano I, Park PJ. Detecting the mutational signature of homologous recombination deficiency in clinical samples. Nat Genet 2019;51:912–9.
15. Telli ML, Jensen KC, Vinayak S, Kurian AW, Lipson JA, Flaherty PJ, et al. Phase II study of gemcitabine, carboplatin, and iniparib as neoadjuvant therapy for triple-negative and BRCA1/2 mutation–associated breast cancer with assessment of a tumor-based measure of genomic instability: PrECOG 0105. JCO 2015;33:1895–901.
16. Isakoff SJ, Mayer EL, He L, Traina TA, Carey LA, Krag KJ, et al. TBCRC009: a multicenter phase II clinical trial of platinum monotherapy with biomarker assessment in metastatic triple-negative breast cancer. J Clin Oncol 2015;33:1902–9.
17. Kaklamani VG, Jeruss JS, Hughes E, Siziopikou K, Timms KM, Gutin A, et al. Phase II neoadjuvant clinical trial of carboplatin and eribulin in women with triple negative early-stage breast cancer (NCT01372579). Breast Cancer Res Treat 2015;151:629–38.
18. Sharma P, Barlow WE, Godwin AK, Pathak H, Isakova K, Williams D, et al. Impact of homologous recombination deficiency biomarkers on

outcomes in patients with triple-negative breast cancer treated with adjuvant doxorubicin and cyclophosphamide (SWOG S9313). Ann Oncol 2018;29:654–60.
19. Mayer EL, Abramson V, Jankowitz R, Falkson C, Marcom PK, Traina T, et al. TBCRC 030: a phase II study of preoperative cisplatin versus paclitaxel in triple-negative breast cancer: evaluating the homologous recombination deficiency (HRD) biomarker. Ann Oncol 2020;31:1518–25.
20. Tutt A, Tovey H, Cheang MCU, Kernaghan S, Kilburn L, Gazinska P, et al. Carboplatin in BRCA1/2-mutated and triple-negative breast cancer BRCAness subgroups: the TNT Trial. Nat Med 2018;24:628–37.
21. Stronach EA, Paul J, Timms KM, Hughes E, Brown K, Neff C, et al. Biomarker assessment of HR deficiency, tumor BRCA1/2 mutations, and CCNE1 copy number in ovarian cancer: associations with clinical outcome following platinum monotherapy. Mol Cancer Res 2018;16:1103–11.
22. Hodgson DR, Dougherty BA, Lai Z, Fielding A, Grinsted L, Spencer S, et al. Candidate biomarkers of PARP inhibitor sensitivity in ovarian cancer beyond the BRCA genes. Br J Cancer 2018;119:1401–9.
23. Ray-Coquard I, Pautier P, Pignata S, Pérol D, González-Martín A, Berger R, et al. Olaparib plus bevacizumab as first-line maintenance in ovarian cancer. N Engl J Med 2019;381:2416–28.
24. Sokol ES, Pavlick D, Khiabanian H, Frampton GM, Ross JS, Gregg JP, et al. Pan-cancer analysis of BRCA1 and BRCA2 genomic alterations and their association with genomic instability as measured by genome-wide loss of heterozygosity. JCO Precis Oncol 2020;4:442–65.
25. Coleman RL, Oza AM, Lorusso D, Aghajanian C, Oaknin A, Dean A, et al. Rucaparib maintenance treatment for recurrent ovarian carcinoma after response to platinum therapy (ARIEL3): a randomised, double-blind, placebo-controlled, phase 3 trial. Lancet 2017;390:1949–61.
26. Färkkilä A, Gulhan DC, Casado J, Jacobson CA, Nguyen H, Kochupurakkal B, et al. Immunogenomic profiling determines responses to combined PARP and PD-1 inhibition in ovarian cancer. Nat Commun 2020;11:1459.
27. Matulonis UA, Wulf GM, Barry WT, Birrer M, Westin SN, Farooq S, et al. Phase I dose escalation study of the PI3kinase pathway inhibitor BKM120 and the oral poly (ADP ribose) polymerase (PARP) inhibitor olaparib for the treatment of high-grade serous ovarian and breast cancer. Ann Oncol 2017;28:512–8.
28. Eikesdal HP, Yndestad S, Elzawahry A, Llop-Guevara A, Gilje B, Blix ES, et al. Olaparib monotherapy as primary treatment in unselected triple negative breast cancer. Ann Oncol 2021;32:240–9.
29. Fisher S, Barry A, Abreu J, Minie B, Nolan J, Delorey TM, et al. A scalable, fully automated process for construction of sequence-ready human exome targeted capture libraries. Genome Biol 2011;12:R1.
30. Yates LR, Gerstung M, Knappskog S, Desmedt C, Gundem G, Van Loo P, et al. Subclonal diversification of primary breast cancer revealed by multiregion sequencing. Nat Med 2015;21:751–9.
31. NCI Genomic Data Commons [Internet]. [cited 2021 May 2]. Available from: https://gdc.cancer.gov/.
32. Ellrott K, Bailey MH, Saksena G, Covington KR, Kandoth C, Stewart C, et al. Scalable open science approach for mutation calling of tumor exomes using multiple genomic pipelines. Cell Syst 2018;6:271–81.
33. Van der Auwera GA, Carneiro MO, Hartl C, Poplin R, Del Angel G, Levy-Moonshine A, et al. From FastQ data to high confidence variant calls: the Genome Analysis Toolkit best practices pipeline. Curr Protoc Bioinformatics 2013;43:11.10.1–11.10.33.
34. Favero F, Joshi T, Marquard AM, Birkbak NJ, Krzystanek M, Li Q, et al. Sequenza: allele-specific copy number and mutation profiles from tumor sequencing data. Ann Oncol 2015;26:64–70.
35. Mermel CH, Schumacher SE, Hill B, Meyerson ML, Beroukhim R, Getz G. GISTIC2.0 facilitates sensitive and confident localization of the targets of focal somatic copy-number alteration in human cancers. Genome Biol 2011;12:R41.
36. Sztupinszki Z, Diossy M, Krzystanek M, Reiniger L, Csabai IN, Favero F, et al. Migrating the SNP array-based homologous recombination deficiency measures to next generation sequencing data of breast cancer. NPJ Breast Cancer 2018;4:16.
37. Knijnenburg TA, Wang L, Zimmermann MT, Chambwe N, Gao GF, Cherniack AD, et al. Genomic and molecular landscape of DNA damage repair deficiency across The Cancer Genome Atlas. Cell Rep 2018;23:239–54.
38. Carter SL, Cibulskis K, Helman E, McKenna A, Shen H, Zack T, et al. Absolute quantification of somatic DNA alterations in human cancer. Nat Biotechnol 2012;30:413–21.
39. Islam SMA, Wu Y, Díaz-Gay M, Bergstrom EN, He Y, Barnes M, et al. Uncovering novel mutational signatures by de novo extraction with SigProfiler-Extractor. bioRxiv 2020;2020.12.13.422570.
40. Campbell PJ, Getz G, Korbel JO, Stuart JM, Jennings JL, Stein LD, et al. Pan-cancer analysis of whole genomes. Nature 2020;578:82–93.
41. D'Andrea AD. Mechanisms of PARP inhibitor sensitivity and resistance. DNA Repair 2018;71:172–6.
42. Li H, Liu Z-Y, Wu N, Chen Y-C, Cheng Q, Wang J. PARP inhibitor resistance: the underlying mechanisms and clinical implications. Mol Cancer 2020;19:107.
43. Ning J-F, Stanciu M, Humphrey MR, Gorham J, Wakimoto H, Nishihara R, et al. Myc targeted CDK18 promotes ATR and homologous recombination to mediate PARP inhibitor resistance in glioblastoma. Nat Commun 2019;10:2910.
44. Jaspers JE, Kersbergen A, Boon U, Sol W, van Deemter L, Zander SA, et al. Loss of 53BP1 causes PARP inhibitor resistance in Brca1-mutated mouse mammary tumors. Cancer Discov 2013;3:68–81.